Available online at www.sciencedirect.com

ScienceDirect

Energy Procedia 50 (2014) 290 – 305

Energy Procedia

The International Conference on Technologies and Materials for Renewable Energy, Environment and Sustainability, TMREES14

Numerical Simulation and Experimental Validation of Integrated Solar Combined Power Plant

A. M. Abdel Dayem[a]*, M. Nabil Metwally[a], A. S. Alghamdi and E.M.Marzouk[b]

Mech. Eng. Dept., College of Engineering and Islamic Architecture, Umm Al-Qura University, Makkah, P.O. 5555, KSA

[a]*Assigned from Faculty of Eng. (Mattaria), Helwan University, Cairo, Egypt*

[b]*Assigned from Faculty of Engineering, Alexandria University, Cairo, Egypt*

Abstract

Combined cycle power plant has the highest efficiency due to recovery heat efficient use. Utilizing solar heating of parabolic troughs can improve the overall efficiency of such plants. Different plants of such technology were successfully installed around the world and one of these plants is the Kurymat plant, which was recently installed south Cairo, Egypt. In the plant the exit flue gases from a gas turbine is used to produce superheated steam into a steam turbine without any supplementary firing. The gas-turbine always works in full load where the steam cycle power is maximized during the day when the solar field performance is maximized. Parabolic trough solar collectors are used to generate the steam during the day time, where the steam mass flow rate is controlled to improve the power produced. A detailed performance model of the integrated combined cycle of Kuraymat plant is created in TRNSYS simulation environment. A numerical simulation of the plant was established and its predicted performance is compared with the measured data of the Kuraymat plant. The numerical results are in close agreement with the measured ones. Annual performance of the validated simulated plant is presented under weather data of Makkah, 21.29 ºN. The power of gas-turbine is improved to 72 MW along the year while the steam-turbine power is increased to about 52 MW that is about 44% of total power. The solar fraction of the plant was estimated at about 25%. The model demonstrates the capability to perform detailed analysis and is very useful for evaluating proposed systems.

Selection and peer-review under responsibility of the Euro-Mediterranean Institute for Sustainable Development (EUMISD)

Keywords: Integrated solar combined cycles; parabolic trough; numerical simulation; TRNSYS software

* Corresponding author. Tel.: +966-2-527-0000; fax: +966-2-527-0027.

E-mail address: amabdeen@uqu.edu.sa

Selection and peer-review under responsibility of the Euro-Mediterranean Institute for Sustainable Development (EUMISD)

doi:10.1016/j.egypro.2014.06.036

1. Introduction

At present time and in the near future term, Solar Thermal Power Plants are going to share scenario-with conventional energy generation technologies, like fossil and nuclear. In such a context, Integrated Solar Combined Cycles (ISCCs) may be an interesting choice since integrated designs may lead to a very-efficient use of the solar and fossil resources. Combined cycle is a way to improve power plant efficiency by utilizing the heat recovery from exhaust gases. If solar energy is used in parallel with this cycle as a renewable and clean source of energy the cycle efficiency will maximized. Tracking parabolic trough collectors have high efficiency in that high level of temperature and are widely used in these plants. Energy storage is not required for this system because those plants are working 24 hours a day. On the other hand direct steam generation can be used efficiently in the steam cycle that is connected in series with the gas-turbine cycle. Direct steam generation (DSG) in parabolic trough collectors causes an increase to competitiveness of solar thermal power plants

Montes et al [1] analyzed Integrated Solar Combined Cycle (ISCC) power plant that consists of a Direct Steam Generation (DSG) parabolic trough field coupled to the bottoming steam cycle of a Combined Cycle Gas Turbine (CCGT) power plant. For this analysis, the solar thermal power plant performs in a solar dispatching mode: the gas turbine always operates at full load, only depending on ambient conditions, whereas the steam turbine is somewhat boosted to accommodate the thermal hybridization from the solar field. Two well-known sites were considered: Almeria (Spain), with a Mediterranean climate, and Las Vegas (USA), with a hot and dry climate. The economic analysis pointed out that this hybrid scheme is a cheaper way to exploit concentrated solar energy, although it is limited to a small fraction of the combined cycle power. The analysis also shows that the marginal cost of solar electricity is strongly influenced by the goodness of coupling, so this cost is lower in Las Vegas than in Almeria.

Niknia and Yaghoubi [2] performed a transient simulation, power expansion of a solar power plant by integrating a new collector and an auxiliary boiler. The new system consists of an oil cycle, a steam cycle and a new extra oil cycle. Comparison of the new system with previous arrangement illustrates that various integration schemes can be easily simulated and an appropriate system to satisfy the main design objectives can be chosen.

In the paper of Cau et al [3], a performance and cost assessment of Integrated Solar Combined Cycle Systems (ISCCSs) based on parabolic troughs using CO2 as heat transfer fluid was reported on. The use of a solar steam generator including only the evaporation section instead of the preheating, evaporation, and superheating sections allows the achievement of slightly better conversion efficiencies. However, the adoption of this solution leads to a maximum value of the solar share of around 10% on the ISCCS power output. The solar conversion efficiencies of the ISCCS systems considered are slightly greater than those of the more conventional Concentrating Solar Power (CSP) systems based on steam cycles (20–23%) and are very similar to the predicted conversion efficiencies of the more advanced direct steam generation solar plants (22–27%).The results of a preliminary cost analysis show that the specific cost of electrical energy produced from solar energy is much greater (about two-fold) than that of electrical energy produced from natural gas.

In work of Rovira et al [4], different ISCC configurations including a solar field based on parabolic trough collectors and working with the so-called Heat Transfer Fluid (HTF) and Direct Steam Generation (DSG) technologies are compared. For each technology, four layouts have been studied: one in which solar heat is used to evaporate part of the high pressure steam of a bottoming Rankine cycle with two pressure levels, another that incorporates a preheating section to the previous layout, the third one that includes superheating instead of preheating and the last one including both preheating and superheating in addition to the evaporation. The authors [5] reveal that the only-evaporative DSG configuration becomes the best choice, since it benefits of both low irreversibility at the heat recovery steam generator and high thermal efficiency in the solar field.

Liu et al [6] investigated the least squares support vector machine (LSSVM) method to model and optimize the parabolic trough solar collector system. Numerical simulations are implemented to evaluate the feasibility and efficiency of the LSSVM method, where the sample data derived from the experiment and the simulation results of

two solar collector systems with 30 m^2 and 600 m^2 solar fields, and the complicated relationship between the solar collector efficiency and the solar flux, the flow rate and the inlet temperature of the heat transfer fluid (HTF) is extracted. Some results indicated the LSSVM method is competent to optimize the solar collector systems.

Nezammahalleh et al [7] considered an integrated solar combined cycle system with DSG technology (ISCCS-DSG), a solar electric generating system (SEGS), and an integrated solar combined cycle system with HTF (heat transfer fluid) technology(ISCCS-HTF). This study showed that levelized energy cost (LEC) for the ISCCS-DSG is lower than the two other cases due to reducing O&M costs and also due to increasing the heat to electricity net efficiency of the power plant. Among the three systems, SEGS has the lowest CO_2 emissions, but it will operate during daytime only.

Baghernejad and Yaghoubi [8] proposed an Integrated Solar Combined Cycle System (ISCCS) as a means of integrating a parabolic trough solar thermal plant with modern combined cycle power plants. Exergy destruction throughout the plant is quantified and illustrated using an exergy flow diagram, and compared to the energy flow diagram. The causes of exergy destruction in the plant include: losses in combustor, collector, heat exchangers, and pump & turbines which accounts for 29.62; 8.69; 9.11 and 8% of the total exergy input to the plant, respectively.

Dersch et al [9] showed four potential projects in India, Egypt, Morocco, and Mexico are considering the ISCCS type solar power cycle configurations. The key questions are when is the ISCCS configuration preferred over the SEGS power cycle configuration and how is the ISCCS plant designed to optimize the integration of the solar field and the power cycle. This paper reviews the results of a collaborative effort under the International Energy Agency SolarPACES organization to address these questions and it shows the potential environmental and economic benefits of each configuration.

2. Kuraymat ISCCS

The hybrid solar power plant in Al Kuraymat (29.27 ºN), Egypt, is among the first in the world. Figure 1 shows an example of an ISCCS with a double-pressure steam turbine and heat recovery steam generator (HRSG). Preheated feed water is drawn from the high pressure pre-heater, evaporated and slightly superheated in the solar steam generator, returned to the HRSG, and together with the steam from the conventional evaporator, finally superheated to the live steam temperature. Steam turbine, preheater, superheater and condenser of an ISCCS have to be larger than the corresponding parts of a simple combined cycle (CC) plant using the same gas turbine type because of the increased steam mass flow for the integrated plant.

The plant near Kuraymat catches solar radiation with a field of parabolic troughs concentrating the heat into a collection tube system filled with circulating heat transfer fluid (HTF) as synthetic thermal oil. This 'solar field' takes up more than 13 acres and has a thermal capacity of 60 MW. The solar collectors are connected in series and parallel to produce the required heat energy by tracking the sun from east to west, rotating on a north-south axis. The parabolic troughs (formed from U shaped glass mirrors) will focus the solar radiation on a system of tubing filled with synthetic oil, which is used as the heat transfer fluid for the solar island. The circulating hot oil is heated to 393 °C at 20 bar and used to evaporate water in heat exchangers. The produced steam is fed into the steam pipework of the heat recovery steam generator. The water/steam and oil cycles are closed systems. The complex character of fluctuating irradiated heat and the severe cyclic operation (the solar field does not deliver any heat during the night) ask for an extraordinary and flexible technology. The heat exchangers should be capable of processing the rapidly progressing temperature of the solar troughs each dawn, while the HRSG has to be both robust and flexible to accept all the generated steam [10].

The steam production is 170 ton per hour at a temperature of 550 °C and a pressure level of 70 bar. The plant has a total installed generating capacity of about 135 MWe. Construction is carried out in such a way that it will be possible to increase the solar component in the future to raise the total installed capacity of the installation to around

150 MWe [11].

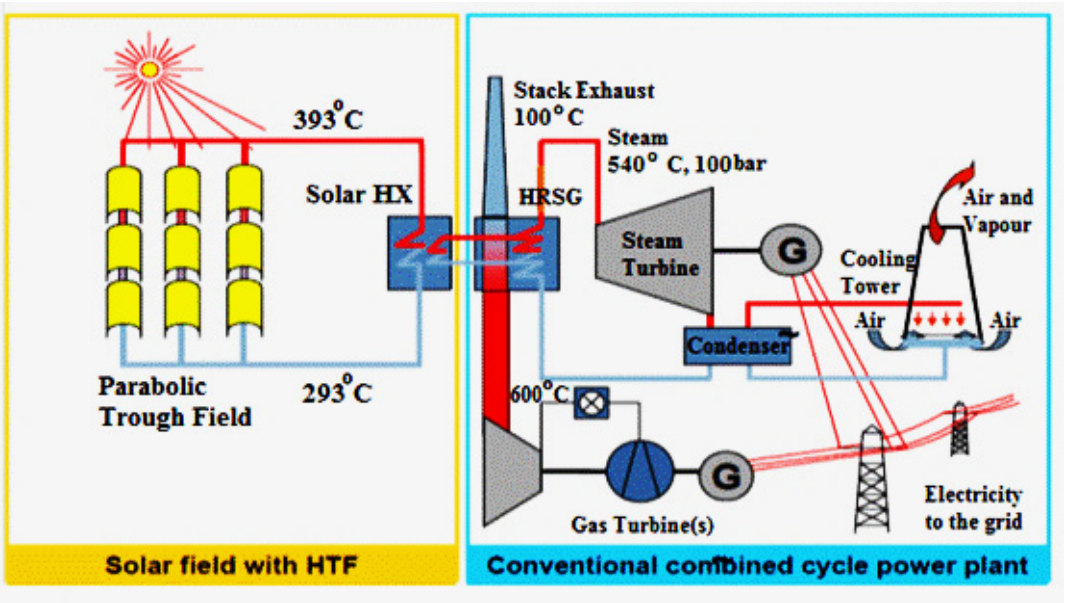

Figure 1: Typical ISCCS Kuraymat solar power plant / Egypt [Fernandez-Garci, 12]

As indicated in Table 1, the solar field consists of 1920 parabolic trough collectors with approximate mirror aperture area of 131000 m^2. It contains 40 collector loops and each loop has 4 completed collectors with 6 collector modules for each. Every 6 collector modules constitute tracking collector. Each two loops are connected in series to obtain high outlet temperature controlled to 393 ºC (evaporation temperature is 400 ºC) where inlet temperature is 293 ºC.

Table 1: Technical data of Solar Island [12]

Description	Value	Unit
Number of Completed Collector Loops	40	-
Number of Completed Collectors per Loop	4	-
Number of Completed Collectors	160	-
Number of Collectors Modules per Completed Collectors	12	-
Number of the whole Collectors Modules	1920	-
Total Effective Mirror Area approximate with 131.000	131000	m^2
HTF Loop Inlet Temperature	293	°C
HTF Loop Outlet Temperature	393	°C
Maximum Solar Field Thermal Energy Output	61	MWt

The 74 MW gas-turbine cycle is an open simple Brayton cycle containing a compressor that produces about 25 bar air flow and a turbine with 74 MW and about 605ºC exhaust gas temperature. The exhaust gases are passed to a heat recovery steam generator (HRSG). The HRSG consists of three economizers, two evaporators and four superheaters. Steam, that exchanges heat with HTF from solar collectors through a heat-exchanger, feeds the HRSG after the second evaporator and enters the second superheater and then to the third and fourth superheaters. The return steam to the solar field is taken from the HRSG after the second economizer. The pumping water from the deaerator enters the first economizer where a part of it is fed to the second economizer and then to the solar field where part of it is fed to the third economizer and then to the second evaporator before mixing with steam coming

from the solar field. The other part is evaporated in the first evaporator and then to the first superheater and then mixing with the outlet steam from high-pressure turbine to the low-pressure turbine [13].

The steam cycle is a Rankine cycle containing a double-pressure heat recovery steam generator (HRSG) that produces a superheated steam into a high-pressure turbine. The exit steam is mixing with a superheated steam coming from the HRSG that is fed to a low-pressure turbine. The exit steam from the low-pressure turbine is condensed in a condenser and then pumped into a deaerator before pumping again into the HRSG.

3. Numerical Simulation

The plant consists of solar field and power cycle. The solar field is parabolic trough collectors, expansion tank, control unit and pumps. On the other hand the power block consists of steam turbine, gas-turbine, air compressor, pumps, heat exchanger, open feed water heater (deaerator), economizer, boiler, superheater and reheater.

TRNSYS-17 program was used to simulate the plant, the details of the program are presented in the manual of the program [14]. TRNSYS is a transient system simulation program with a modular structure. A system is defined in TRNSYS to be a set of components, interconnected in such a manner as to accomplish a specified task. The software consists of different subroutines and each subroutine simulates a component of the system. Because the system consists of components, it is possible to simulate the performance of the system by collectively simulating the performance of the interconnected components. In the following subsections the governing equations for each system component are illustrated.

3.1. Solar Field

The modeling of the solar-field includes parabolic-trough collector, control unit, expansion tank and pump with neglecting the loss through connecting pipes. Estimating of solar radiation and collector shading effect is also considered.

1. Parabolic-trough Collector

The model attempts to alleviate both issues of inlet and outlet temperatures based on the local temperature of the fluid. The model assumes that the fluid in the absorber tube is divided into a number of iso-volumetric sections (nodes) with each section of absorber tube (node) having unique temperatures and fluid properties that change with temperature (and therefore with time).The governing differential equation that describes the temperature of the fluid in one of these nodes as a function of time can be written as:

$$\frac{d(mu)}{dt} = \dot{Q}_{absorbed} + \dot{Q}_{fluid,in} - \dot{Q}_{losses} - \dot{Q}_{fluid,out} \quad (1)$$

Where $$\frac{d(mu)}{dt} = m\frac{du}{dt} + u\frac{dm}{dt} \quad (2)$$

If $$m = \rho.V\ ,\ \rho = r_0 + r_1T + r_2T^2\ and\ u = u_0 + u_1T + u_2T^2 \quad (3)$$

By differentiation and rearranging the left side of the equation it can get

$$\frac{d(mu)}{dt} = (mu_1 + 2mu_2T + ur_1V + 2r_2uVT)\frac{dT}{dt} \quad (4)$$

$$\dot{Q}_{absorbed} = AG_{beam}IAMf_{endloss}f_{mirror}f_{dust}f_{bellows}\tau_{glass}\alpha_{coating}f_{misc} \quad (5)$$

$$f_{endloss} = 1 - \frac{F\tan(\theta)}{L} \quad (6)$$

Where *fmirror*- a factor which accounts for the geometric inaccuracies of the reflect mirror (1 = perfect mirror)
fdust- a factor which accounts for dust on the glass receiver tube (1 = no dust)

fbellows- a factor which accounts for the shading of the mirror by the collector bellows (1 = no shading)
fmisc- a factor which accounts for misc. losses from the collection system (1 = no misc. losses)
τglassc- the transmittance of the receiver glass to solar radiation (1 = perfect transmission)
αcoating- the absorptance of the coating on the absorber tube (1 = all incident radiation absorbed)
F - focal length of collector, θ – incidence angle
L- length of single panel collector

$$\dot{Q}_{fluid,in} = \dot{m}_{in} h_{in} \tag{7}$$

$$\dot{Q}_{fluid,out} = \dot{m}_{out} h_{out} \tag{8}$$

$$\dot{m}_{out} = \dot{m}_{in} - \frac{dm}{dt} = \dot{m}_{in} - V(r_1 + 2r_2 T)\frac{dT}{dt} \tag{9}$$

$$\dot{Q}_{losses} = U_L(T - T_{ambient}) \tag{10}$$

$$\text{Where } U_L = \frac{a_0 + a_1 T + a_2 T^2 + a_3 T^3 + DNI(a_4 + a_5 T^2)}{W(T-25)} \tag{11}$$

Where W is aperture mirror width. Equation (1) is solved numerically to find dT/dt (or ΔT/Δt in numerical solution) to estimate the temperature of the next time level which equals T+ΔT.

2. Variable Speed Pump

It operates in such a way that when ON (control signal input set greater than 0.5), the volumetric and mass flow of fluid through the pump is determined by the intersection point of the system curve and the pump head curve that is closest to a user specified "desired mass flow rate". It is able to interpolate between curves provided for specific pump speeds and match the user specified desired pump flow rate. γ is a normalized mass flow rate for which a value of 0 corresponds to no flow, and a value of 1 corresponds to the pump's rated flow (control signal). "H_p" is the normalized system head with a value of H_p indicating zero head and a value of 1 indicating rated head.

$$H_p = a_0 + a_1\gamma + a_2\gamma^2 + a_3\gamma^3 + \cdots \tag{12}$$

$$\text{And } T_{out} = T_{in} + \dot{Q}_f / \dot{m} \;\; C_p \tag{13}$$

$$\text{Where } \dot{Q}_f = \dot{P}_{shaft}\left(1 - \eta_p\right) + (\dot{P} - \dot{P}_{shaft}) f_m \tag{14}$$

$$\text{And } \dot{P}_{shaft} = \dot{m} \;\; \Delta p / \rho \;\; \eta_p \tag{15}$$

3. Control Unit

Signal of the control unit (γ) that switches the solar-filed pump is a function of solar radiation. That is because to shut down the pump where there is no solar radiation and after testing it can be written as

$$\gamma = MIN[1, MIN\left(0.73, (0.035 * G_{beam})\right)] \tag{16}$$

4. Expansion Tank

This subroutine models a variable volume, fluid-filled storage tank where the properties of the fluid are assumed to change with temperature. The tank is assumed to be fully mixed and stratification in the storage tank is not considered.

$$\frac{d(mu)}{dt} = \dot{Q}_{in} - \dot{Q}_{losses} - \dot{Q}_{out} \tag{17}$$

$$\text{Then} \qquad \frac{dT}{dt} = \frac{-\dot{m}_{in} u + \dot{m}_{out} u + \dot{m}_{in} h_{in} + \dot{m}_{out} h_{out} - U_L SA(T - T_a)}{(mu_1 + 2mu_2 T)} \tag{18}$$

=change in the average temperature of the tank with time

$$\text{Where } h = h_0 + h_1 T + h_2 T^2 \tag{19}$$

When ΔT is estimated the temperature of the next layer can be found as T+ΔT.

5. Estimation of Solar Radiation

The data files distributed with TRNSYS 17 were generated using Meteonorm [15]. All files were generated using default options in Meteonorm V 5.0.13. The weather and radiation data is based on monthly values of Makkah that Meteonorm generates stochastically to hourly values [15].

6. Collector Array Shading

Shading can be characterized by the fraction of the collector area that is blocked by a neighboring collector row in the direction of the sun. *W*a is the width of the parabolic collector, *D*a is the distance between axes, β is the slope of the collectors and βap is the slope of the plane that contains the collector axes. In order to maximize beam radiation, it is necessary that the sun be in a plane that is perpendicular to the collector aperture and that contain the receiver axes. For a single row of collectors, the fraction of the aperture area shaded by an adjacent row of collectors neglecting edge effects, is given by

$$f_{bs,1} = \max(\left(1 - \frac{P}{W_a}\right), 0) \tag{20}$$

Where *P* is the distance between the collector axes on a projection that is normal to a line from a collector axis to the sun. If θp is the angle between a plane containing the sun and an axis and a plane that is perpendicular to the plane which contains the collector axes, *P* is found from

$$P = D_a \cos(\theta_p) \quad \text{where} \qquad \theta_p = \beta - \beta_{ap} \tag{21}$$

The overall fraction of array area that is shaded at any point in time is given in terms of the shaded fraction for a single row of collectors and the number of rows, N_R, as

$$f_{bs} = (N_R - 1) f_{bs,1} / N_R \tag{22}$$

The incident beam radiation (G_{beam}) is then

$$G_{beam} = (1 - f_{bs}) DNI \tag{23}$$

3.2 Power Cycle

Steam that is generated from the steam generator (economizer, evaporator and superheater) flows to high-pressure and low-pressure turbines. From there it is expanded to a condenser and pumped to a deaerator to the steam generator again. Considering these components the governing equations are presented.

1. Economizer

This component models a pre-heater for steam condensate using the heat exchanger effectiveness approach [15]. The effectiveness is a measure of the heat transfer at the inlet fluid conditions to the maximum possible heat transfer given the fluid inlet conditions. In this model, the inlet hot-side fluid attempts to heat a flow of steam condensate to a user-specified temperature just below the condensate saturation temperature. The device is assumed to be off if either of the flow rates is zero, if the inlet hot-side fluid temperature is below the inlet condensate temperature, or if the inlet condensate temperature is already above the desired condensate outlet temperature.

2. Boiler and Superheater

This component models both heat recovery steam generator (HSRG) and superheater; a device which uses high-temperature solar heat to heat a steam flow. This model will attempt to meet the user-specified steam outlet condition but may be limited by the entering hot-side temperatures and flow rate. This device may operate in a counter-flow configuration. The model relies on the pinch-point temperature difference approach [16] to check for impossible (or unrealistic) heat exchange conditions. The pinch-point temperature difference is defined to be the minimum temperature difference between the hot-source fluid and the steam that allows for heat transfer between the fluids. The pinch-point is checked at the outlet of the steam flow (inlet of the hot source flow), the outlet of the hot source flow (the steam inlet), at the steam saturated liquid point, and at the steam saturated vapor point. If the temperature difference at these points is less than the pinch-point temperature difference, the heat transfer is re-calculated such that the pinch-point problem is not encountered. The device is assumed to be off if either of the flow rate inlets is zero, or if the inlet steam enthalpy is already at or above the desired outlet steam enthalpy.

This version of the heat recovery steam generator calculates the maximum steam flow rate which can be produced given the inlet hot-side source conditions and the desired steam outlet enthalpy; constrained by the specified pinch-point. In this model, the inlet steam flow rate is not used and is just provided for continuity.

3. Steam Turbine

This model simulates a non-condensing steam turbine that takes a user-specified inlet steam flow and calculates the total electrical load that the turbine can meet. Next, an inlet steam mass flow is assumed and the initial guess is the inlet mass flow minus the extraction mass flows. The model then proceeds with a series of calculations for each stage of the turbine. The TRNSYS steam properties subroutine is called with the inlet entropy and the outlet pressure. The returned enthalpy is the ideal enthalpy for the expansion. The actual enthalpy after expansion is obtained from:

$$h_{out,a} = h_{in} - \eta_T(h_{in} - h_{out,s}) \tag{24}$$

The work performed during expansion at the current stage is given by:

$$\dot{W} = \dot{m}_{T,in}(h_{in} - h_{out,a}) \tag{25}$$

4. Condenser

This component models a condenser for steam applications where the condensing pressure is known and provided to the model as an input. This model calculates the resultant heat transfer and outlet steam conditions given the desired degrees of subcooling leaving the condenser (provided by the user). The outlet steam pressure is set to the condensing pressure even when the flow rate is zero to avoid convergence problems in components that rely on this model to set the back-pressure for the steam flow loop. A steam condenser is essentially a heat exchanger that cools steam while heating water or some other liquid stream. It calls the TRNSYS steam properties subroutine with inlet steam temperature and pressure to check the values of the other properties and to determine the quality of inlet steam. The degrees of subcooling are then applied:

$$T_{out} = T_{sat} - \Delta T_{subcool} \tag{26}$$

The energy given up during condensing is given by:

$$\dot{Q}_{cond} = \dot{m}(h_{in} - h_{out}) \tag{27}$$

5. Pump

This component models a steam condensate pump. The user specifies the inlet steam condensate conditions and the desired outlet pressure and the model calculates the theoretical power from a compressed liquid calculation. The enthalpy of steam exiting the device is determined from an energy balance:

$$h_{out} = h_{in} + \frac{\dot{Q}}{\gamma \dot{m}_{rtd}} \quad (28)$$

6. Dearator

This component models an open steam heater in which high-temperature steam at a variable flow-rate is mixed with low-temperature steam at a known flow-rate in order to elevate the low-temperature steam to a user-specified outlet condition. This component calculates the flow rate of high-temperature steam required to meet the desired outlet conditions; bounded by a user-defined maximum high-temperature steam flow rate [17]. This component also models an open feedwater heater in which saturated or superheated steam is mixed with sub-cooled condensate in order to bring the temperature of the condensate at or near its saturation temperature. This component will calculate the required steam flow rate in order to meet the user-specified outlet condition. The high-temperature steam flow rate is set to zero if the low-temperature steam enthalpy is already above the desired outlet enthalpy or if the high-temperature steam is at a lower enthalpy than the low-temperature steam inlet. The high-temperature steam flow rate is set to the user-defined maximum mixing flow rate if the enthalpy of the high-temperature steam is above the inlet low-temperature steam enthalpy and below the desired outlet enthalpy. This device is assumed to be perfectly insulated.

7. Air Compressor

The model assumes that the gas behaves like an ideal gas with constant but average properties. The average specific heat of the air stream is calculated from an integrated correlation based on the inlet and outlet temperatures of the air stream. The ideal outlet temperature is calculated using ideal gas relationships and then the actual outlet temperature is found using the provided efficiency. With the outlet temperature known, the required power can be found.

8. Combustion Device

This component models a simple heat addition device for a gas-turbine system. The combustion process is simply modeled as a heat gain to the air with a user-defined efficiency. Increasing in air mass causing by the products of combustion is ignored in this model. The air is assumed to act like an ideal gas with constant (but average) properties. The average specific heat of the air stream is calculated from an integrated correlation based on the inlet and outlet temperatures of the air stream. The outlet temperature is set to the desired set-point temperature if the capacity of the machine is not exceeded in doing so. If the capacity of the machine is reached, the device will run at its capacity and the resultant outlet temperature calculated.

9. Gas Turbine

The average specific heat of the air stream is calculated from an integrated correlation based on the inlet and outlet temperatures of the air stream. The theoretical power produced is calculated from an ideal gas relationship using the inlet and outlet pressures. The actual power is then found by multiplying the theoretical power by the user-supplied efficiency and the outlet air conditions then found.

3.3 Numerical Solution of Equations

The above components are interconnected together to estimate the different outputs. The hourly measured metrological data were used as an input. The data includes the total and diffuse solar radiation and the ambient temperature. The governing equations were solved together to find the different variables included in them. The unknown variables include the temperatures and flow rates at the inlets and outlets of each component. Moreover,

the useful heat gain and heat losses can be estimated that are the inputs of the economic analysis. In the following sections the results of the simulation are discussed.

The above governing equations were solved dependently together using the TRNSYS 17 program [14]. The modified Euler method was used to solve the equations using pre-defined time step 0f 1.0 h and the convergence accuracy was checked in each time step to limit the number of iterations into 30.

4. Experimental Validation of Numerical Simulation

To validate the numerical simulation, Kuraymat plant was simulated and predicted performances were compared with measured data under the same conditions of design, specifications and weather. The measured data are obtained from the plant acquisition system that records weather conditions and plant performance in real time. The data includes the weather data of direct normal irradiance, ambient temperature, wind speed and relative humidity. The data of plant record the power, temperature and mass flow rate of both gas and steam turbines, and HTF.

Figure 2 presents a comparison between predicted and measured power of both gas and steam turbines for September 3 – 4, 2013. As shown in the figure the power of the steam turbine is improved during the day when the solar radiation is maximized. In that case the mass flow rate is increased while the steam temperature is relatively constant as shown in Fig. 3. Regarding the gas –turbine the predicted power is not widely changed, it depends only on the ambient temperature and atmospheric pressure where the measured one is widely changed from night to the day. That variation is due to change the temperature as in Fig. 3 and it is no reason for that. In general the predicted power of gas turbine is in close agreement with the measured one during the day.

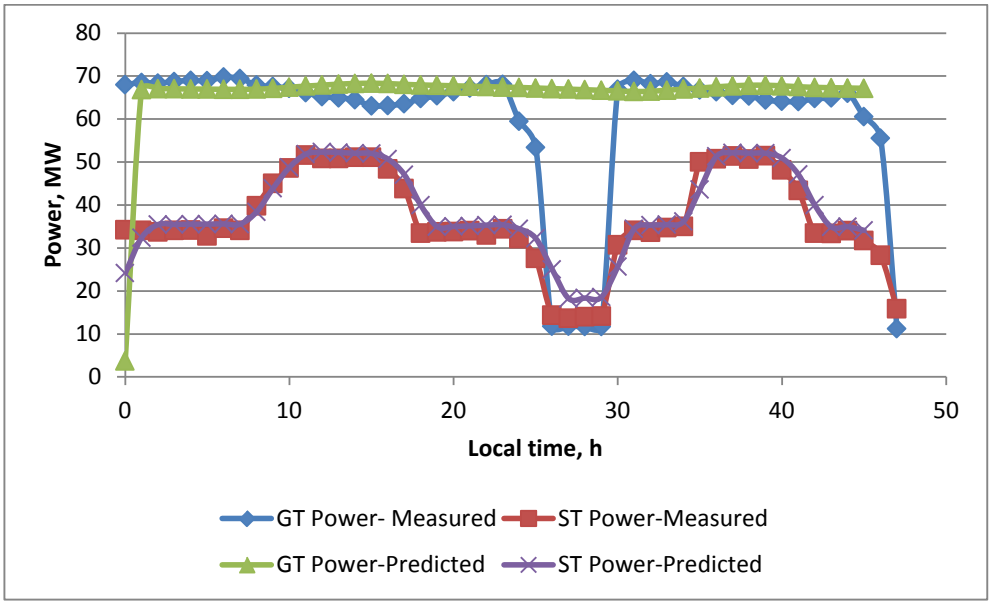

Figure 2: Comparison between measured and predicted power of both gas and steam turbines for September 3 – 4, 2013

As illustrated in Fig. 3 the inlet temperature of both gas and steam turbines seems constant along the day. The measured inlet temperature of the gas turbine is about 610 ºC where the predicted is about 590 ºC. This difference is obtained due to ignoring any losses or deficiencies in the numerical simulation. There is no reason for dropping the temperature of about 60 ºC during night. The direct normal solar irradiance is obtained in Fig. 4 for both predicted and measured values for the same days of comparison. The agreement seems good except few hours of cloudy weather during the second day. Therefore the predicted weather data by Meteonorm program to be used in

performance estimation is highly recommended.

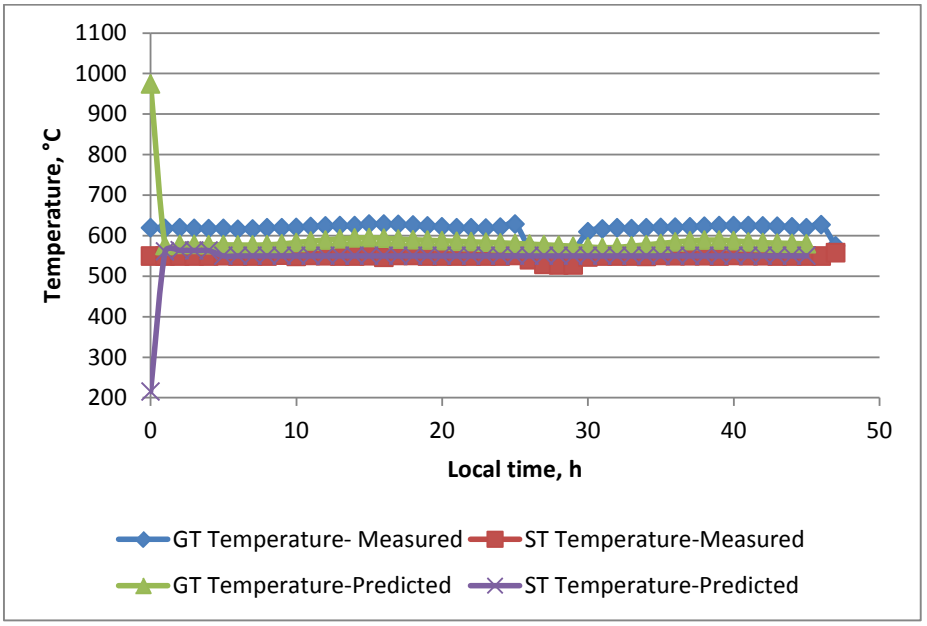

Figure 3: Comparison between measured and predicted inlet temperature of both gas and steam turbines for September 3 – 4, 2013

The predicted HTF temperature and flow rate are compared with the measured values as in Fig. 5. The predicted values for both the temperature and mass flow rate are in close agreement with the measured ones during the sun shining where there is a difference for the temperature during night. The measured temperature is higher than predicted one during the night, may be due to the HTF is heated to not lower the temperature under 200 ºC.

5. **Prediction of Annual Performance of the Solar Power Plant at Makkah**

Under the weather conditions of Makkah, KSA (21.29 ºN), where higher solar radiation and ambient temperature along the year are existed, solar power plant can have more efficiency and power. Therefore the integrated solar combined power plant with the same design and characteristics of the Kuraymat plant was simulated under the weather conditions of Makkah. The annual performance of the plant is estimated and the hourly data are predicted according to the above mathematical model and hourly weather data of DNI and ambient temperature.

The power for both gas and steam turbines is estimated hourly along a year as shown in Fig. 6. The power of gas-turbine is around 70 MW along the year with slightly improvement during the summer when the ambient temperature is maximized. The gas-turbine power is higher than that found for the same plant under Kuraymat weather conditions as shown in Fig. 2 by about 5%. On the other hand the steam-turbine power is changed from 43 MW during the evening and night to 52 MW during sun-shine where it is lowered to 33 MW during few hours in night as proposed in the plant operation control. Between those values the power is varied depending on the weather conditions of clouds and dust, and due to longer day-time period during summer than in winter. That result can be clearly presented in Fig. 8 where the DNI is obtained low.

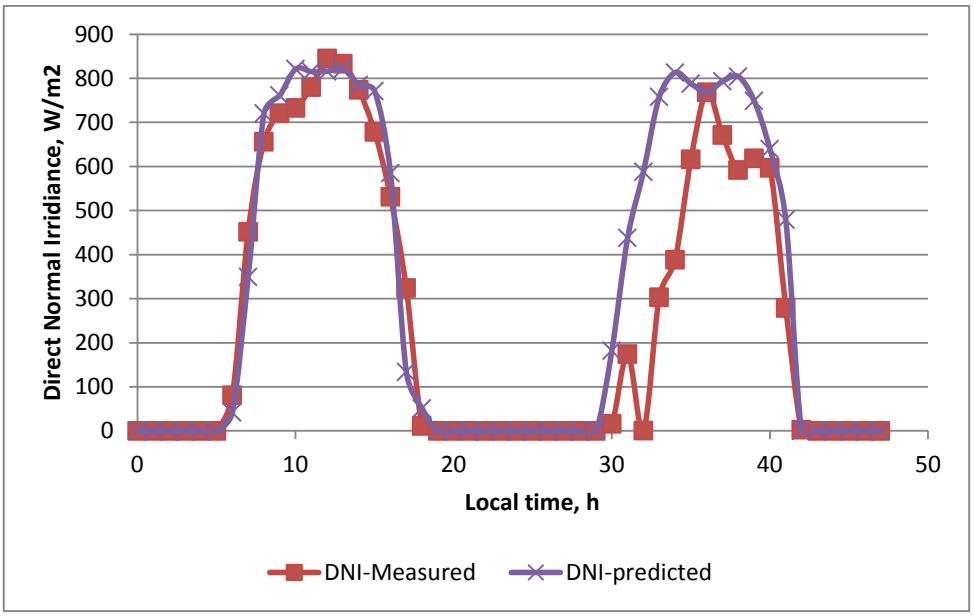

Figure 4: Comparison between measured and predicted direct normal irradiance (DNI) for September 3 – 4, 2013

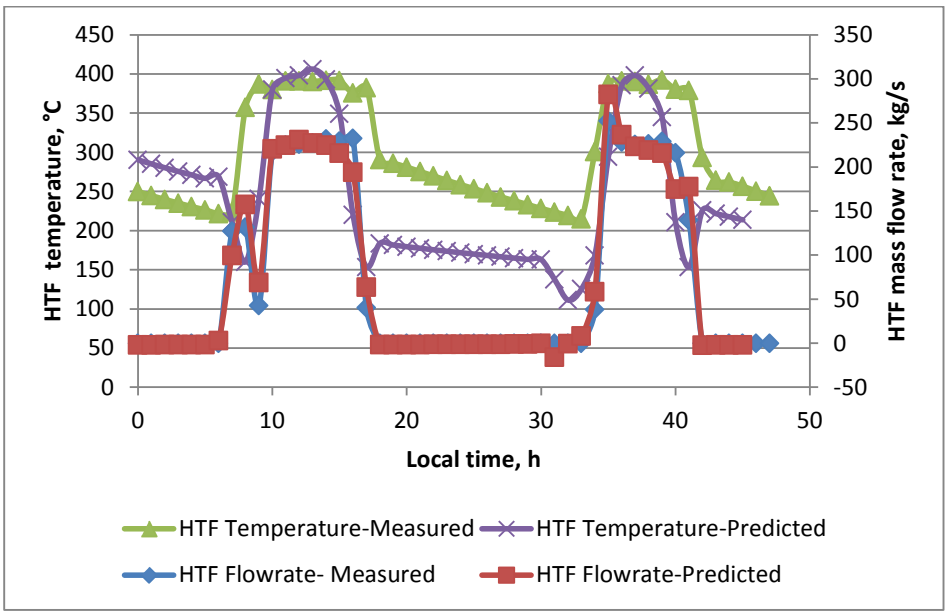

Figure 5: Comparison between measured and predicted data of both HTF temperature and flow rate for September 3 – 4, 2013

In Fig. 7 the temperature variation of both gas and steam turbines is the same as the power variation. The gas turbine temperature is relatively constant and it is around 605 ºC as proposed. The slight difference is coming from the ambient temperature. Similarly the steam-turbine inlet temperature is varied between 180ºC during few hours in night as explained to above 550 ºC as the set point considered in the design, while some fluctuations occurred during the cloudy hours.

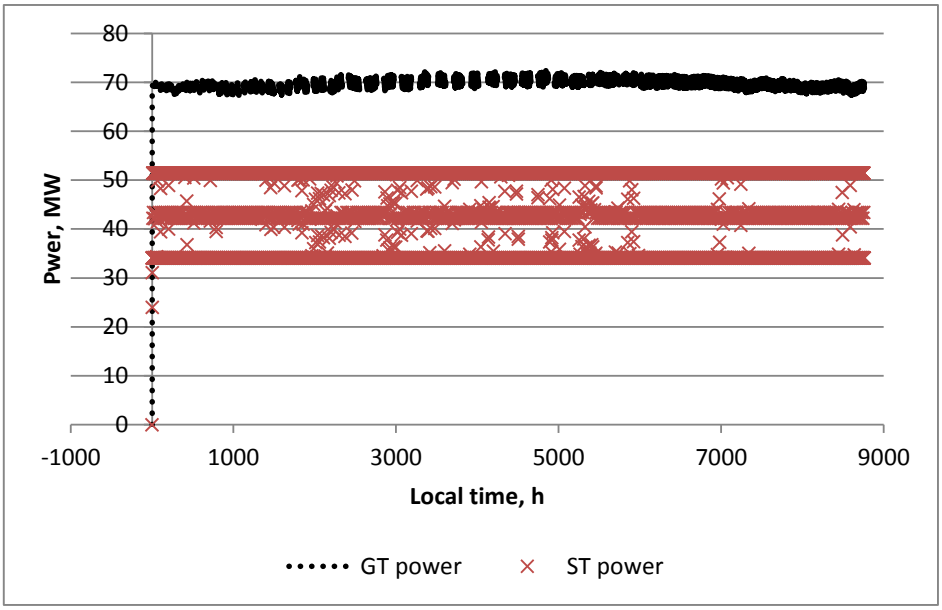

Figure 6: Annual hourly variation of predicted power of both gas and steam turbines for a proposed ISCCS power plant at Makkah, KSA

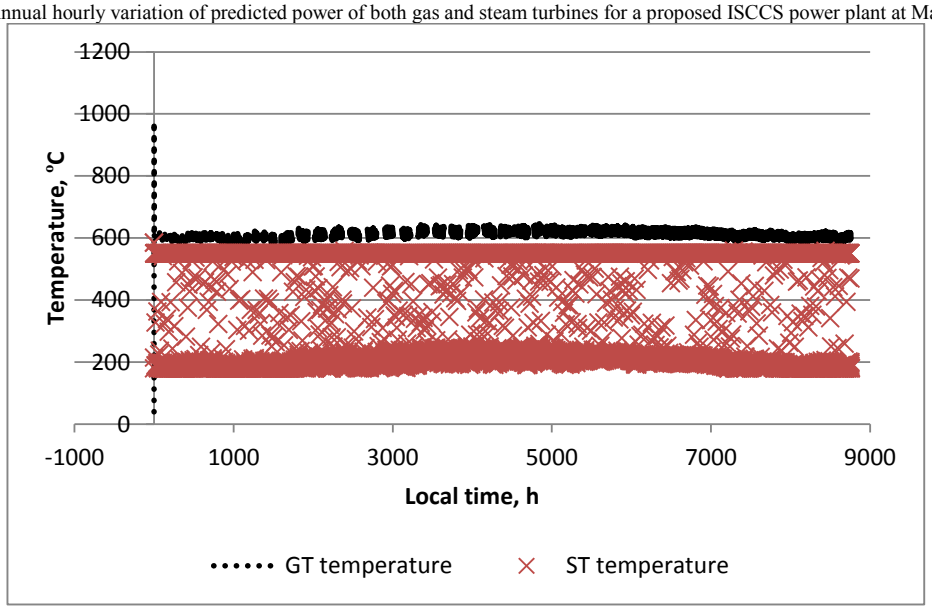

Figure 7: Annual hourly variation of predicted inlet temperature of both gas and steam turbines for a proposed ISCCS power plant at Makkah, KSA

Figure 8 illustrates the DNI variation along the year. The DNI seems fine along the year and it has high values during the winter, spring and autumn. In summer the DNI is lower than other months with more cloudy periods. In general the DNI is more enough to obtain high output temperature from the parabolic-trough solar collectors along the year as shown in Fig. 9.

The HTF outlet temperature is estimated as shown in Fig. 9 with mass flow rate. As discussed above the temperature reaches about 450 ºC during autumn months and sometimes in spring months where it is not lower than 400 ºC in summer with the maximum allowable mass flow rate. The minimum mass flow rate indicated in the figure is considered to avoid freezing of the HTF during night.

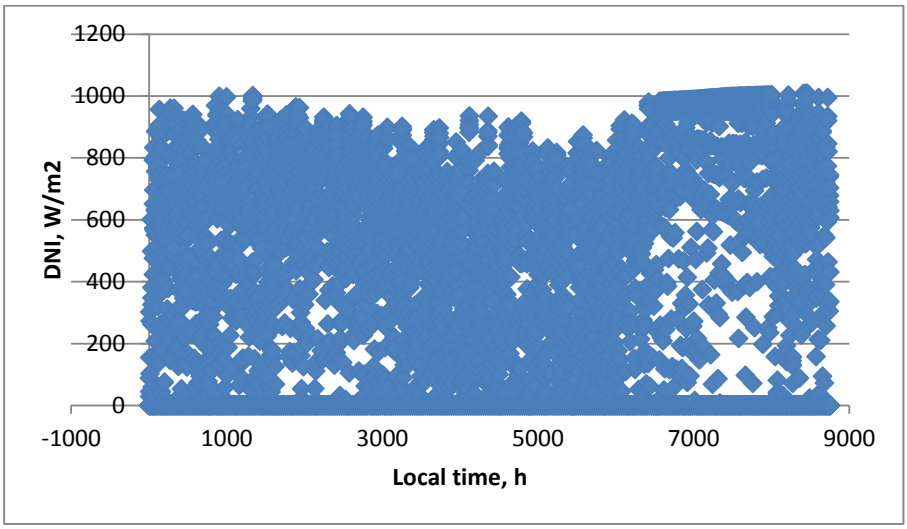

Figure 8: Annual hourly variation of predicted direct normal solar irradiance on Makkah, KSA

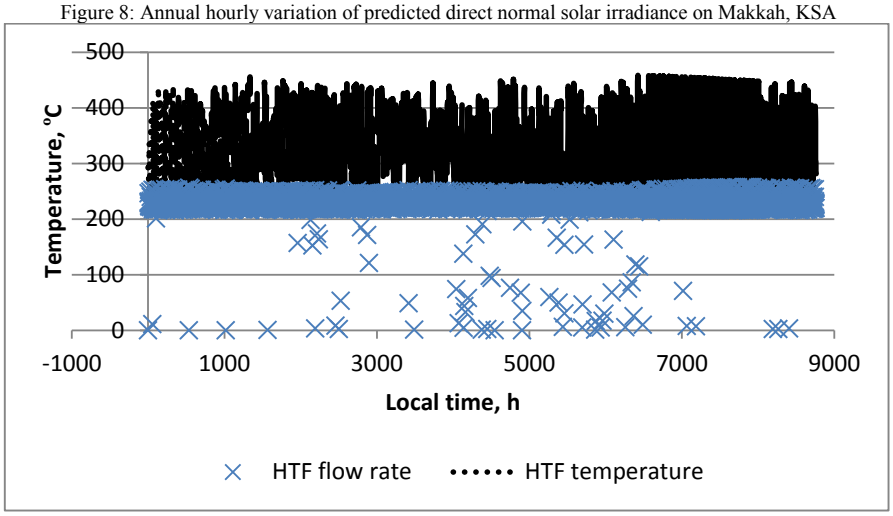

Figure 9: Annual hourly variation of predicted HTF temperature and mass flow rate, for a proposed ISCCS power plant at Makkah, KSA

The solar fraction is defined as the ratio of useful heat gain from the solar field to the total energy generated from the plant. It is estimated hourly for the plant along a year as shown in Fig. 10. It is ranged about 27% for the sunny days along the year. Therefore it is improved in Makkah as proposed in the design stage which it was proposed as 10 %. The solar fraction is lowered under cloudy weather while it equals zero during night as normally expected. As expected, because the direct normal solar irradiance is the only heat source to the solar field, the hourly annual variation is similar to the DNI variation. The solar fraction seems high for major hours during Winter, Autumn and Spring while it is lower during the Summer with more cloudy weather. In general the share fraction of the solar energy is good and if it is required to be improved, one the solution is increasing of the collector area.

6. Conclusion

Numerical simulation of integrated combined solar power plant was developed and validated by experimental measured data from Kuraymat plant, Egypt. The same plant is visualized under the weather conditions of Makkah, KSA, 21.29 ºN. In general, at Makkah the plant performance is improved and the gas-turbine power generated is

increased by about 5% due to high ambient temperature while the steam-turbine power is improved by about 10 % along the year due to the higher DNI and the average solar fraction is about 25%. The temperature of both turbines and HTF is presented with successful solar energy utilization in this sector. It is obtained that the plant can be successfully and efficiently installed in KSA as additional potentiality of the electrical power generation sector, with high feasibility.

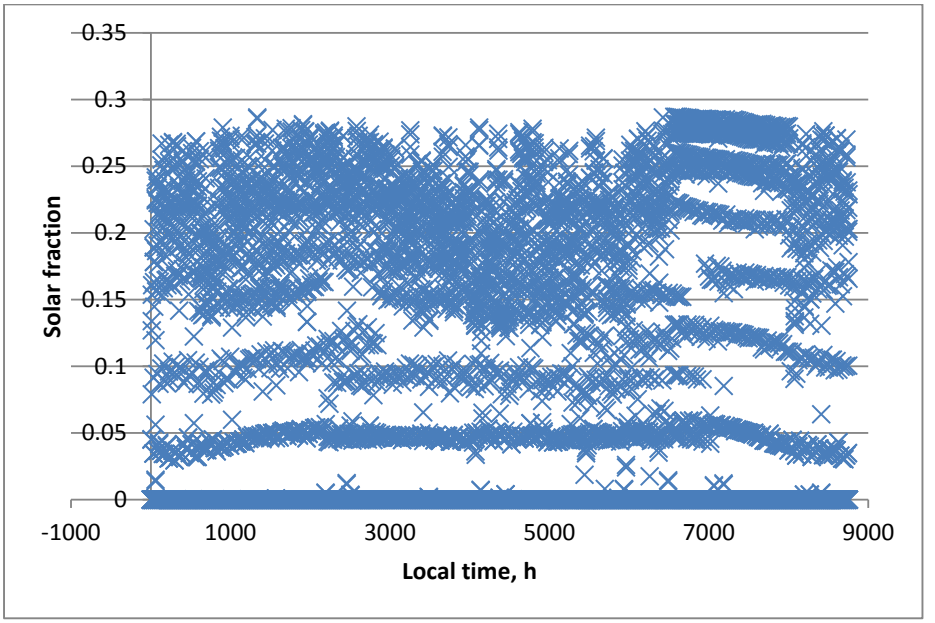

Figure 10: Annual hourly variation of predicted solar fraction for a proposed ISCCS power plant at Makkah, KSA

Acknowledgment

The authors would thank 'Saudi Center of Research Excellence in Renewable Energy/KFUPM' for appreciate funding of this study and following up of the project steps. Also great thank to Eng. Ayman Fayek, NREL, Egypt and Eng. Moustafa Abdel-Moneam, Ministry of Electricity, Egypt for their cooperation to get information and measured data from the plant.

Nomenclatures

$a_0, a_1, a_2,..$	Polynomial coefficients in the system head curve	SA	tank surface area for thermal loss calculations
A	The area formed by the mouth of the parabolic reflector	t	Time
Cp	Specific heat of fluid	T	temperature of fluid
f_m	Fraction of pump motor inefficiencies that contribute to a temperature rise in the fluid stream passing through the pump. The remainder of these inefficiencies contributes to an ambient temperature rise.	u	coefficient in the correlation of internal energy of the fluid
H	coefficient in the enthalpy correlation of the fluid as a function of temperature	U_L	heat transfer coefficient
IAM	The Incidence Angle Modifier; a dimensionless parameter that accounts for the collector's change in the transmittance absorptance product when the sun is not normal to the plane of the collector.	V	Fluid volume
G_{beam}	The amount of beam solar radiation incident on the plane of the collector surface.	$\dot{W}$	The work performed during expansion in a

given turbine stage.

m	mass of fluid	**Symbols**	
$\dot{m}$	Fluid mass flow rate	Δp	Pump pressure rise
$\dot{m}_{T,in}$	The mass flow rate of steam entering a given stage of the turbine.	ΔT	A temperature difference.
$\dot{m}_{rtd}$	Rated mass flow rate of the pump	Δt	the TRNSYS time step
$\dot{Q}_{cond}$	The rate at which energy is transferred from the steam to the cooling liquid flow.	γ	Normalized mass flow rate (desired flow rate / rated flow rate) or control signal
$\dot{Q}$	Energy transferred.	η_p	Efficiency of pumping the fluid
$\dot{P}$	Power drawn by the pump.	η_T	The isentropic efficiency of the turbine.
r	coefficient in the density correlation of the fluid as a function of temperature	ρ	Density of fluid

References

[1] Montes M.J, Rovira A, Mueoz M, Martnez-Val JM. Performance analysis of an Integrated Solar Combined Cycle using Direct Steam Generation in parabolic trough collectors. Applied Energy 88 (2011); 3228–3238

[2] ImanNiknia, MahmoodYaghoubi. Transient simulation for developing a combined solar thermal power plant. Applied Thermal Engineering 37 (2012); 196-207

[3] Giorgio Cau, Daniele Cocco, Vittorio Tola, "Performance and cost assessment of Integrated Solar Combined Cycle Systems (ISCCSs) using CO2 as heat transfer fluid", Solar Energy 86 (2012) 2975–2985

[4] Antonio Rovira, María José Montes, Fernando Varela, Mónica Gil. Comparison of Heat Transfer Fluid and Direct Steam Generation technologies for Integrated Solar Combined Cycles. Applied Thermal Engineering 52 (2013); 264-274

[5] Abdel Dayem A M, Nabil Metwally M, Alghamdi A S and Marzouk E M. Potential of Solar Thermal Energy Utilization in Electrical Generation. 2nd International Conference on Energy Systems and Technologies 18 – 21 Feb. 2013, Cairo, Egypt

[6] Qibin Liu, Minlin Yang, Jing Lei, Hongguang Jin, ZhichaoGao, Yalong Wang. Modeling and optimizing parabolic trough solar collector systems using the least squares support vector machine method. Solar Energy 86 (2012); 1973–1980

[7] Nezammahalleh H, Farhadi F, Tanhaemami M. Conceptual design and techno-economic assessment of integrated solar combined cycle system with DSG technology. Solar Energy 84 (2010); 1696–1705

[8] Baghernejad A, Yaghoubi M. Exergy analysis of an integrated solar combined cycle system. Renewable Energy 35 (2010); 2157-2164

[9] Juergen Dersch, Michael Geyer, Ulf Herrmann, Scott A. Jones, Bruce Kelly, Rainer Kistner, Winfried Ortmanns, Robert Pitz-Paal,Henry Price. Trough integration into power plants-a study on the performance and economy of integrated solar combined cycle systems. Energy 29 (2004); 947–959

[10] http://www.solarpaces.org/Tasks/Task1/egypt_kuraymat.htm

[11] http://www.nrel.gov/csp/solarpaces/project_detail.cfm/projectID=65

[12] Fernandez-Garci A, Zarza E, Valenzuel L, M. Perez. Parabolic-trough solar collectors and their applications. Renewable and Sustainable Energy Reviews 14 (2010); 1695–1721

[13] Personal contact with Eng. AymanFayek, NREL, Egypt

[14] Trnsys home page: www.trnsys.com

[15] Meteotest (2003). Meteonorm handbook, Parts I, II and III. Meteotest, Bern, Switzerland, http://www.meteotest.ch

[16] Incropera, Frank P., and DeWitt, David P. Fundamentals of Heat and Mass Transfer. 5th edition. New York: John Wiley and Sons, Inc., 2002.

[17] El-Wakil, M. M. Powerplant Technology. New York: McGraw-Hill, Inc., 1984.